Available online at www.sciencedirect.com
SCIENCE DIRECT
ELSEVIER
Journal of the European Ceramic Society 26 (2006) 1463–1471
ECERS
www.elsevier.com/locate/jeurceramsoc

Synthesis of glass–ceramics in the CaO–MgO–SiO_2 system with B_2O_3, P_2O_5, Na_2O and CaF_2 additives

D.U. Tulyaganov [a], S. Agathopoulos [a], J.M. Ventura [a], M.A. Karakassides [b], O. Fabrichnaya [c], J.M.F. Ferreira [a,*]

[a] *Department of Ceramics and Glass Engineering, University of Aveiro, CICECO, 3810-193 Aveiro, Portugal*
[b] *Department of Materials Science and Engineering, University of Ioannina, GR-45110 Ioannina, Greece*
[c] *Max Planck Institut fuer Metallforschung, Heisenbergstr 3, D-70569 Stuttgart, Germany*

Received 30 November 2004; received in revised form 13 February 2005; accepted 19 February 2005
Available online 25 March 2005

Abstract

Glass–ceramics based on the CaO–MgO–SiO_2 system with limited amount of additives (B_2O_3, P_2O_5, Na_2O and CaF_2) were prepared. All the investigated compositions were melted at 1400 °C for 1 h and quenched in air or water to obtain transparent bulk or frit glass, respectively. Raman spectroscopy revealed that the main constituents of the glass network are the silicates Q^1 and Q^2 units. Scanning electron microscopy (SEM) analysis confirmed liquid–liquid phase separation and that the glasses are prone to surface crystallization. Glass–ceramics were produced via sintering and crystallization of glass-powder compacts made of milled glass-frit (mean particle size 11–15 μm). Densification started at 620–625 °C and was almost complete at 700 °C. Crystallization occurred at temperatures >700 °C. Highly dense and crystalline materials, predominantly composed of diopisde and wollastonite together with small amounts of akermanite and residual glassy phase, were obtained after heat treatment at 750 °C and 800 °C. The glass–ceramics prepared at 800 °C exhibited bending strength of 116–141 MPa, Vickers microhardness of 4.53–4.65 GPa and thermal expansion coefficient (100–500 °C) of 9.4–10.8 × 10^{-6} K^{-1}.

Keywords: Sintering; Crystallization; Microstructure-final; Glass; Glass–ceramics

1. Introduction

Glass–ceramics exhibit particular interest for several applications, such as thermal, chemical, biological and dielectric ones, because these systems provide great possibilities to manipulate their properties, such as transparency, strength, resistance to abrasion, coefficient of thermal expansion, through the control of the composition, extent of crystallization, crystal morphology, crystal size and aspect ratio. The easy of fabrication techniques in conjunction with lower production cost offer additional advantages.[1–4] The synthesis of the parent glass is an important step of the development of the final glass–ceramic material because the principal components and their proportion in the glass composition govern the precipitation of the crystalline phases. The results of this process endow the resultant glass–ceramic with the desired properties.

In the CaO–MgO–SiO_2 system, glass–ceramics of diopside, wollastonite, and melilite have been thoroughly investigated.[5–9] Provided that appropriate nucleating agents are incorporated in suitable amounts, earlier studies have demonstrated that crystallization of diopside and wollastonite-based glass–ceramics advances via a bulk crystallization mechanism.[1–5] In the CaO–MgO–SiO_2 system, the first stage of crystallization occurs via separation of phases, rich in divalent metal oxides and having relatively simple crystal structures, primarily diopside-type solid solutions. The effect of crystallization-stimulating additions may result from several mechanisms. For example, Cr_2O_3 remarkably increases the crystallization rate only for Fe-containing compositions as the corresponding mechanism includes

* Corresponding author. Tel.: +351 234 370242; fax: +351 234 425300.
E-mail address: jmf@cv.ua.pt (J.M.F. Ferreira).

0955-2219/$ – see front matter © 2005 Elsevier Ltd. All rights reserved.
doi:10.1016/j.jeurceramsoc.2005.02.009

formation of spinels, which, in turn, actively catalyse the formation of pyroxene phases.[2,5,10,11] The catalytic effect of fluorides in pyroxene-based systems is due to the intensification of phase separation in the liquid phase, associated with an enrichment of the segregated zones with the pyroxene component. As a result, diopside-type solid solutions are formed in the fluoride-containing compositions at the first stage of crystallization. The stimulating effect of titania additions in pyroxene systems was found insufficient.[12–14] In the case of melilite and wollastonite glass–ceramics, it has been found that sulphides of Fe, Mn and Zn as well as fluorides might promote successful bulk crystallization.[2,15]

Good mechanical and chemical properties of glass–ceramic materials in the $CaO–MgO–SiO_2$ system have indicated these materials as suitable for use in wear resistant, thermo-mechanical, biomedical[1,5,16–18] and ceramic-coating applications.[19,20] Nevertheless, the relatively elevated processing temperatures (e.g. for glass-melting or for devitrification) characterize this family of materials. Obviously, high energy consumption opposes the current global trends related to environmental and economic issues.

This work aimed to produce high quality glass–ceramics in the $CaO–MgO–SiO_2$ system based on diopside and wollastonite at temperatures lower than those reported in earlier studies. To achieve this goal, the basic composition of the parent glass, 51–52% SiO_2, 37–39% CaO and 9–12% MgO (all the compositions are referred to wt.%, unless otherwise stated), was selected in the low temperature region of the liquidus surface of the ternary system close to the composition of the liquid in the invariant equilibrium of the transition type (i.e. 51.4% SiO_2, 36.8% CaO, 11.8% MgO)

$$\text{liquid} + \text{pseudowollastonite} \rightleftarrows \text{akermanite} + \text{wollastonite} \quad (1)$$

and of the eutectic type (i.e. 51.6% SiO_2, 35.6% CaO, 12.8% MgO)[21]

$$\text{liquid} \rightleftarrows \text{wollastonite} + \text{diopside} + \text{akermanite} \quad (2)$$

Furthermore, with respect to the selected basic compositions of the parent glasses (i.e. considering them as 100%), limited amounts of auxiliary fluxes were incorporated, specifically 5.7–6.2% B_2O_3, 3.3–3.8% P_2O_5, 5.0–5.5% Na_2O and 6.5–7.0% CaF_2.

In this work, three compositions were investigated, designated hereafter as 1, 2 and 3, with chemical compositions presenting in the Table 1. These compositions feature a practically constant ratio among the fluxes but the total content of the fluxes gradually decreases from the composition 1–3 from 19.31% to 16.39%, respectively. To allow the reader to understand the behaviour of these materials to a maximum extent and therefore to assess them for applications, a wide range of features and properties of the produced materials is presented.

Table 1
Chemical compositions of the investigated glasses 1, 2 and 3 (in wt.%)

Glass	SiO_2	B_2O_3	CaO	MgO	P_2O_5	Na_2O	CaF_2
1	41.39	5.33	30.05	9.25	3.26	4.74	5.98
2	42.23	4.89	31.54	8.50	2.99	4.36	5.49
3	42.95	4.52	32.80	7.86	2.77	4.03	5.07

2. Materials and experimental procedure

Powders of silicon oxide and calcium carbonate (with purity >99.5%), and H_3BO_3, $4MgCO_3{\cdot}Mg(OH)_2{\cdot}5H_2O$, Na_2CO_3, CaF_2, and $NH_4H_2PO_4$ (with purity >99.9%) were used. Homogeneous mixtures of batches (∼100 g), obtained by dry mixing for 0.5 h in a high-speed porcelain ball mill (Nannetti, Faenza, Italy), were preheated at 1000 °C for 1 h for decarbonisation and then melted in Pt crucibles at 1400 °C for 1 h, in air.

Glasses in bulk form were produced by casting of melts on preheated bronze moulds and subsequent immediate annealing at 600 °C (i.e. close to the transformation temperature T_g) for 1 h. To test the crystallization of these bulk glass samples, heat treatments at 700 °C, 800 °C and 900 °C for 1 h were carried out.

Glasses in frit form were obtained by quenching the melts in cold water. The frits were dried and then dry milled in a high-speed porcelain ball mill for 0.5 h (Nannetti, Faenza, Italy; balls/material weight ratio was approximately 1.5). The particle size distribution of the powders was similar (the mean particle size was almost the same: 11.3, 14.6 and 13.5 μm for the powders 1, 2 and 3, respectively). The glass powders were granulated (by stirring in a mortar) in a 5 vol.% polyvinyl alcohol solution (PVA, Merck; the solution of PVA was made by dissolution in warm water) in a proportion of 98.5 wt.% of frit and 1.5 wt.% of PVA solution. Rectangular bars with dimensions of 4 mm × 5 mm × 50 mm were prepared by uniaxial pressing (80 MPa). The bars were sintered at four different temperatures, 700 °C, 750 °C, 800 °C and 850 °C. The soaking time at the sintering temperatures was 1 h, while a slow heating rate of 2–3 K/min aimed to prevent deformation of the samples.

In this study, the following techniques and apparatus were employed. The structural analysis of the produced glasses was done at the surface of bulk glasses by Raman spectroscopy (micro Raman system, Renishaw 1000, UK) using the 532 nm line of a solid state laser at 60 mW for excitation. Raman scatter was collected by means of a microscope (Leica, UK) equipped with lenses 50× and 100×. The particle size distribution of the powders of the frits was determined by light scattering technique (Coulter LS 230, UK, Fraunhofer optical model). Glass powders were used for differential thermal analysis (DTA, Labsys Setaram TG-DTA/DSC, France, heating rate 5 K/min, in air). Annealed bulk glass blocks, as-pressed glass-powder compacts and sintered rectangular blocks of glass–ceramics were used for dilatometry measurements (Bahr Thermo

Analyse DIL 801 L, Germany, heating rate 5 K/min; cross section of samples 4 mm × 5 mm). The crystallized phases were identified by X-ray diffraction (XRD, Rigaku Geigerflex D/Mac, C Series, Cu Kα radiation, Japan). Scanning electron microscopy (SEM, Hitachi S-4100, Japan) equipped with energy dispersive spectroscopy apparatus (EDS) was employed for microstructure observations and elemental analysis at polished (final stage of polishing 1 μm diamond paste) and etched (by immersion in 2 vol.% HF solution for 1–4 min) surfaces. Archimedes' method (i.e. immersion in ethylenoglycol) was employed to measure the apparent density of the annealed glasses and the sintered glass–ceramic bars. The mechanical properties were evaluated by measuring Vickers microhardness (Shimadzu microhardness tester type M, Japan, load of 9.8 N; each value is the mean value of measurements made with five samples, with 10 indentations for each sample) and three-point bending strength of rectified parallelepiped bars (3 mm × 4 mm × 50 mm) of sintered glass–ceramics (Shimadzu Autograph AG 25 TA, 0.5 mm/min displacement; the results are the average of measurements made on, at least, 12 bars). Water absorption was measured according to the ISO-standard 10545-3, 1995, i.e. weight gain of dried bulk samples after immersion into boiling water for 2 h, cooling for 3 h and sweeping of their surface with a wet towel. The linear shrinkage during sintering was calculated from the difference of the dimensions between the green and the resultant sintered samples.

3. Results

3.1. Glasses

The three compositions were completely melted at 1400 °C after 1 h and the melts were easily cast, resulting in transparent and colourless glasses with no visible crystalline inclusions, as was also confirmed by X-ray and SEM analyses afterwards.

The microstructure of the three annealed (at 600 °C) glasses (1, 2, 3) was similar. Evidences of liquid–liquid phase separation were clearly observed (Fig. 1a). Droplets of segregated liquid phase, seemingly sorted in two groups of bigger (oval shaped, marked with (i)) and smaller droplets (like tiny spots, marked with (ii)), were homogenously distributed in the glass matrix.

The Raman spectra of the investigated glasses (Fig. 2) are similar and feature a dominant band at about 958 cm^{-1}, a shoulder at its high frequency side at ∼1040 cm^{-1}, bands at 648 cm^{-1}, ∼880 cm^{-1}, a broad band envelope double peaking at 340 cm^{-1} and 440 cm^{-1} and a number of bands with weak intensity at 580 cm^{-1}, 780 cm^{-1} and 1450 cm^{-1}. The assignment of these peaks is presented in Section 4.

The dilatation curves (Fig. 3) shows that the transition point (T_g) of the investigated glasses ranged between 585 °C and 590 °C and their softening point (T_s) between 625 °C and 640 °C. From the slope of the linear part of these plots

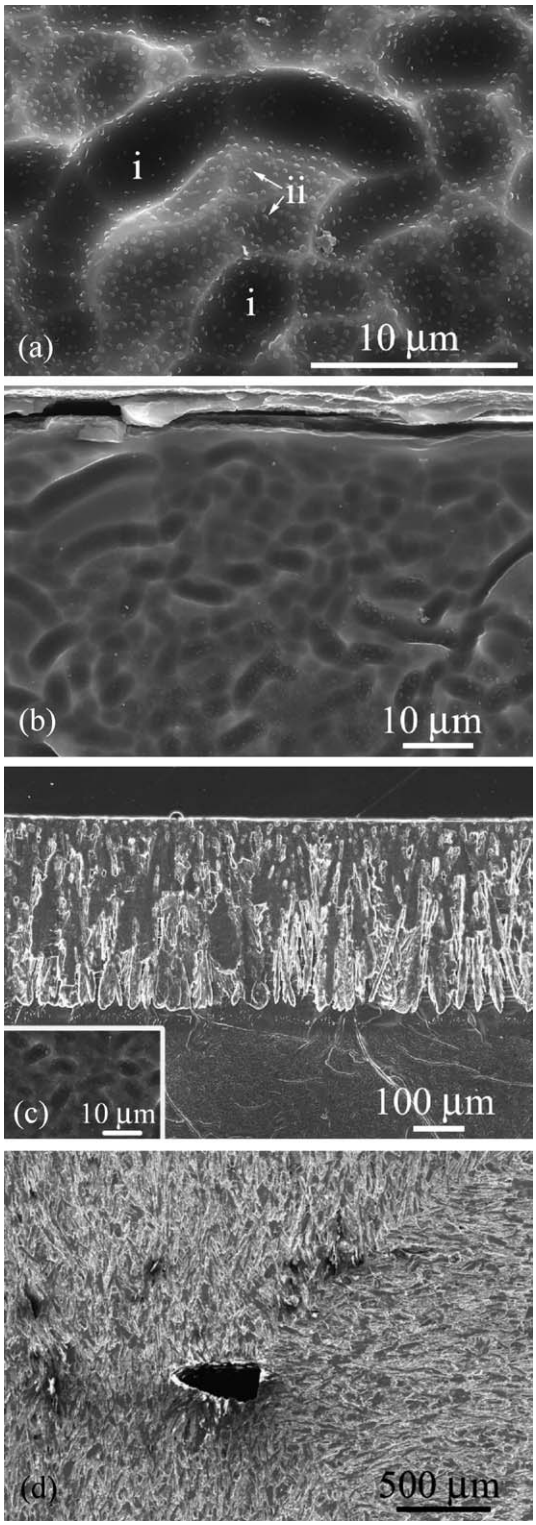

Fig. 1. Microstructure of the annealed bulk glass 1 (a), which comprised bigger (oval shaped, marked with (i)) and smaller droplets (like tiny spots, marked with (ii)), and its evolution after 1 h heat treatment at 700 °C (b), 800 °C (c), the outer surface of the sample is at the top of the image and the inset shows the bulk of the glass at higher magnification), and 900 °C (d), observed by SEM at secondary electron mode after etching of polished surfaces with 2% HF solution (there were not striking differences among the microstructures of the three investigated glasses).

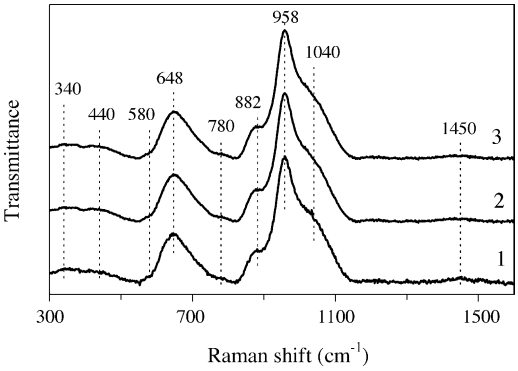

Fig. 2. Raman spectra of the investigated glasses.

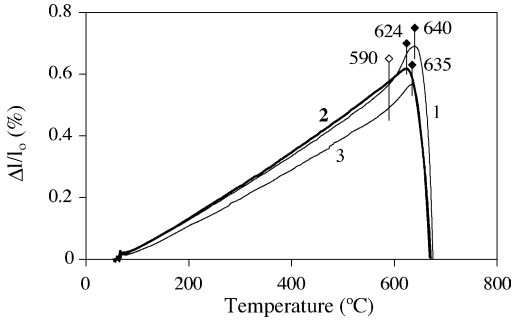

Fig. 3. Dilatation curves of bulk annealed glasses.

between 100 °C and 500 °C, the thermal expansion coefficients (CTE) of the glasses 1, 2 and 3 were calculated as $10.3 \times 10^{-6}\,K^{-1}$, $10.7 \times 10^{-6}\,K^{-1}$ and $9.18 \times 10^{-6}\,K^{-1}$, respectively.

A single strong exothermic peak, attributed to crystallization, was registered in the differential thermal analysis (DTA), which was slightly shifted towards higher temperatures from the glass 1 to the glass 3 (Fig. 4).

Finally, the density of the annealed (at 600 °C) glasses was 2.87 g/cm^3 for all the investigated glasses.

3.2. Crystallization of bulk glasses

The evolution of microstructure of the bulk glasses heat treated at different temperatures is presented in the Fig. 1b–d

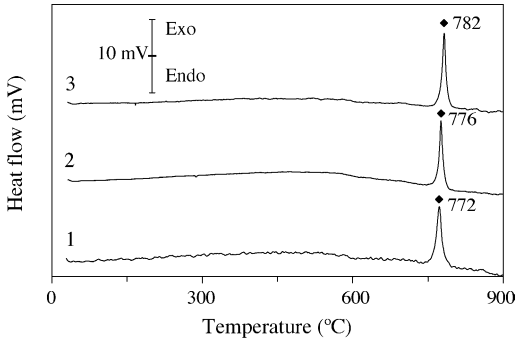

Fig. 4. Differential thermal analysis (DTA) of glass-powders (the mean particle size pf the powders is reported in the text).

(there were not striking differences among the microstructures of the three investigated glasses). After heat treatment at 700 °C (Fig. 1b), the effect of phase separation was more pronounced than in the annealed glass (Fig. 1a), since the bigger droplets are obviously more dispersed, but there was still no evidence of crystallization. The microstructure of the bulk glasses heat treated at 800 °C (Fig. 1c) unequivocally confirms that the glasses are prone to surface crystallization. Crystal growth advances towards the core of the bulk glass and after heat treatment at 900 °C the crystallization process has been completed (Fig. 1d).[7,9] Although there were no striking morphological differences of the crystals of different phases, our EDS analyses in conjunction with the aid of SEM images of the reference[7] allow us to assign wollastonite to acicular shaped crystals and pyroxene to dendritic ones. The advancement of crystal growth from the surface to the core probably caused the formation of few large and small voids in the bulk of the glass–ceramics, observed after the completion of crystallization at 900 °C (Fig. 1d).

3.3. Glass–ceramics from glass-powders compacts

The crystallization temperatures of the glass-powder compacts (i.e. 700 °C, 750 °C, 800 °C, 850 °C) were chosen considering the temperatures of glass transition (i.e. 585–590 °C, Fig. 3), the exothermic peak of crystallization (i.e. 772–782 °C, Fig. 4), and the results of dilatometry measurements of as-pressed glass-powder compacts (plots are not shown), which demonstrated that sintering starts at 620–625 °C, which is higher than T_g.

The influence of the temperature of heat treatment on the appearance of the samples and their crystallinity is presented in Figs. 5 and 6, respectively. Completely dense samples of dark grey colour but of amorphous nature were obtained at 700 °C, indicating that sintering should precede crystallization. Devitrification starts at higher temperatures. Diopside, wollastonite and akermanite were identified in the X-ray spectra after heat treatment at 750 °C (the former two phases were the dominant ones). The same assemblage of phases was registered in the XRD spectra of samples heat treated at 800 °C. White colour and high degree of densification characterized the samples heat treated at 750 °C and 800 °C.

Table 2 shows the influence of firing temperature on shrinkage, density and bending strength. Increase of firing

Fig. 5. Appearance of glass-powder compacts made of composition 1 after heat treatment at different temperatures for 1 h.

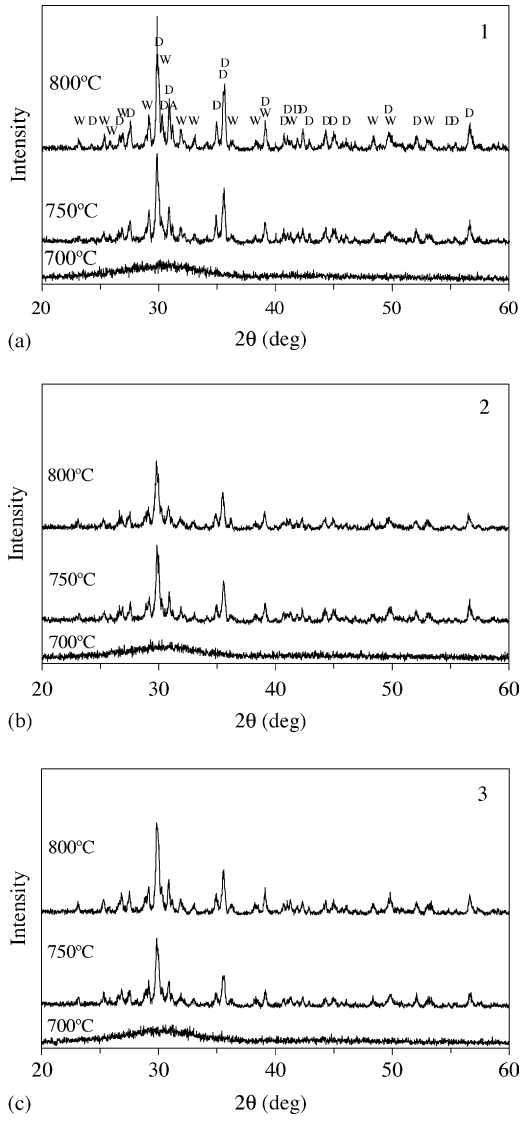

Fig. 6. XRD spectra of glass-powder compacts heat treated at different temperatures for 1 h. A, akermanite, ($Ca_2MgSi_2O_7$, 35-0592); W, β-wollastonite ($CaSiO_3$, 42-0550); D, diopside ($CaMgSiO_6$, 78-1390) (the intensities have not been normalised; full scale of intensity axis 1800 cps).

Table 2
Properties of samples made of glass-powder compacts heat treated at different temperatures for 1 h

Property	Composition	Temperature (°C)		
		700	750	800
Shrinkage (%)	1	14.1 ± 0.3	14.5 ± 0.1	13.6 ± 0.2
	2	13.9 ± 0.3	13.5 ± 0.2	13.4 ± 0.2
	3	13.8 ± 0.1	13.6 ± 0.3	13.6 ± 0.2
Density (g/cm^3)	1	2.87 ± 0.01	2.85 ± 0.01	2.84 ± 0.01
	2	2.82 ± 0.01	2.93 ± 0.01	2.90 ± 0.01
	3	2.81 ± 0.01	2.88 ± 0.01	2.86 ± 0.01
Bending strength (MPa)	1	90 ± 9	108 ± 6	116 ± 5
	2	80 ± 11	134 ± 5	141 ± 11
	3	78 ± 10	138 ± 11	139 ± 8

temperature to 850 °C caused gradual decrease of density and shrinkage and development of visible bubbles underneath the surface of the samples. Consequently, the optimum values of properties of the investigated materials were achieved after heat treatment at 750–800 °C.

Table 3 supplements Table 2 with the values of microhardness, water absorption and coefficient of thermal expansion of glass–ceramics heat treated at 800 °C for 1 h, while Fig. 7 presents their microstructure. Well-defined big prismatic crystals and smaller acicular ones were embedded in glassy matrix. The prismatic crystals were highly packed and significantly bigger in the glass–ceramics 2 (Fig. 7b) and 3 (Fig. 7c) than in 1 (Fig. 7a). Elemental EDS analyses allow us to assign the big crystals to diopside and the

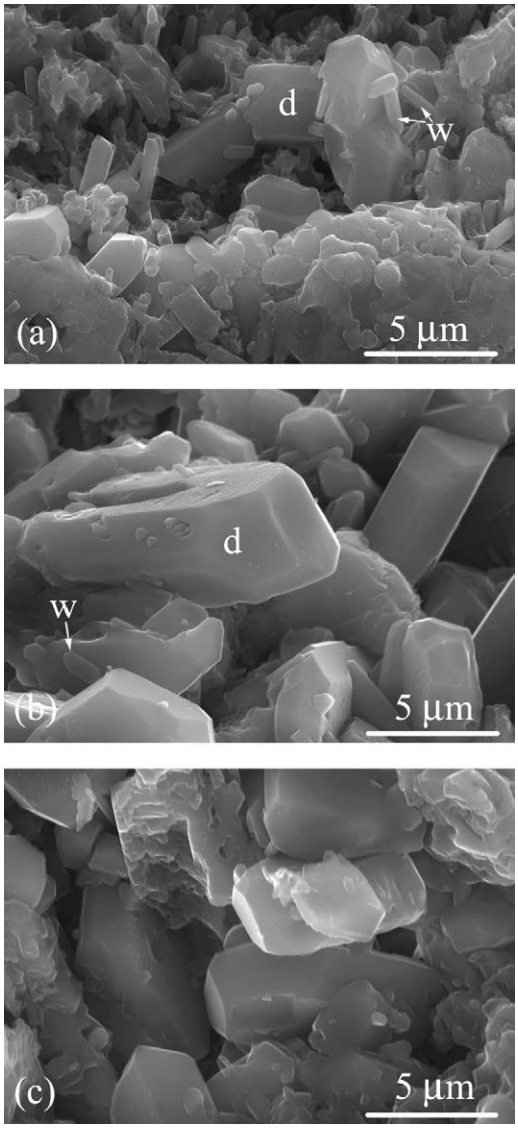

Fig. 7. Typical microstructures of glass-powder compacts made of the compositions 1 (a), 2 (b) and 3 (c) heat treated at 800 °C for 1 h, observed by SEM at secondary electron mode after etching of polished surfaces with 2% HF solution. The crystals assigned to diopside and wollastonite are marked with d and w, respectively.

Table 3
Properties of samples made of glass-powder compacts heat treated at 800 °C for 1 h

Property	Composition		
	1	2	3
Microhardness (GPa)	4.53 ± 0.35	4.61 ± 0.30	4.65 ± 0.40
Water absorption (%)	0.16 ± 0.02	0.15 ± 0.02	0.17 ± 0.02
Coefficient of thermal expansion 100–500 °C (10^{-6} K^{-1})	9.4	10.8	10.3

small ones to wollastonite (marked with d and w in Fig. 7, respectively). However, with respect to stoichiometric diopside and wollastonite, the crystals assigned to diopside featured a slight excess in Ca, while the crystals assigned to wollastonite featured a slight deficiency of Si. The above deviations from stoichiometry might indicate formation of solid solutions, whose exact composition could not be accurately determined due to the big size of the EDS spot (about 1 μm) comparing to the small size of the crystals.

4. Discussion

The experimental results of this study demonstrated the added B_2O_3, Na_2O, P_2O_5 and CaF_2 in the quantities used act as favourable fluxes for glasses but did not favour bulk crystallization. The glasses were prone to surface crystallization, which subsequently resulted in formation of large crystals (>100 μm) and a coarse microstructure (Fig. 1c and d). Therefore, the production of good quality glass–ceramic materials was addressed to the processing via glass-powder compacts, owing to the fact that doping with B_2O_3, P_2O_5 and CaF_2 favours densification of compacts of glass-powders.[19,22,23] The microstructure and the crystallinity of the resultant glass–ceramics should be related to the structural features of the parent glasses.

The Raman spectra suggest that the investigated glasses have similar structures (Fig. 2). The assignment of the peaks was done following guidelines of earlier studies on alkali and alkaline earth silicate,[24–29] borate[30–32] and phosphate glasses.[33] The most important features of the structure of the investigated glasses are summarized as follows. The bands at 958 cm^{-1} and 882 cm^{-1} can be assigned to Si–O^- stretching in silicate units with 2 and 3 non-bridging oxygens (NBOs) (Q^2 and Q^1), respectively. The shoulder at 1040 cm^{-1} is assigned to Si–O^0 vibrations of bridging oxygens in silicate units contain NBOs (Q^2, Q^1 and Q^3). The concentration of Q^3 units is probably low because the Si–O^- stretching vibrations of Q^3 units, which occur at about 1100 cm^{-1}, appear to have very weak intensity. The bands between 550 cm^{-1} and 750 cm^{-1} are attributed to the Si–O–Si bending vibrations in the various silicate units. Especially the band at ~650 cm^{-1} is attributed to Si–O–Si bending motions in Q^2 units whereas the high frequency asymmetry of this band is assigned to analogous vibrations of Q^1 units. The weak bands at 780 cm^{-1} and 1450 cm^{-1} can be attributed to vibrations of borate units and the bands at 580 cm^{-1} and 440 cm^{-1} to the O–P–O bending modes of the orthophosphate PO_4^{3-} unit (Q^0). The P–O^- symmetric stretching vibrations of the PO_4^{3-} units are expected at 958 cm^{-1} and therefore they should also affect the band intensity in this frequency region that is attributed to vibrations of Q^2 silicate units.

The structural units of the glass network, which were predominantly Q^1 and Q^2, should be related to the crystalline phases of diopside, wollastonite and akermanite, developed in the glass matrix after heat treatment (Fig. 6). It is well known that $[Si_2O_7]^{6-}$ dimers (i.e. Q^1 units) constitute sorosilicates, such as akermanite, while single chains of the general formula $[SiO_3]^{2-}$ (i.e. Q^2 units) are the main structural elements of pyroxene and pyroxenoids.[1,34] As it was previously discussed, phase separation (Figs. 1a and b) has seemingly stimulated the formation of crystalline phases.[1–4]

Fig. 8 shows the isothermal section of the sub-solidus CaO–MgO–SiO_2 phase diagram, calculated at 800 °C using the database of Huang et al.[35] If we neglect B_2O_3, P_2O_5, Na_2O and CaF_2, then the three investigated compositions correspond to the points marked by the triangles in the diagram. According to the calculations, the assemblage of the thermodynamically stable phases is the same for all the investigated compositions and temperatures (i.e. wollastonite, diopside and akermanite). Table 4 presents the weight proportions of these phases calculated in the equilibrium

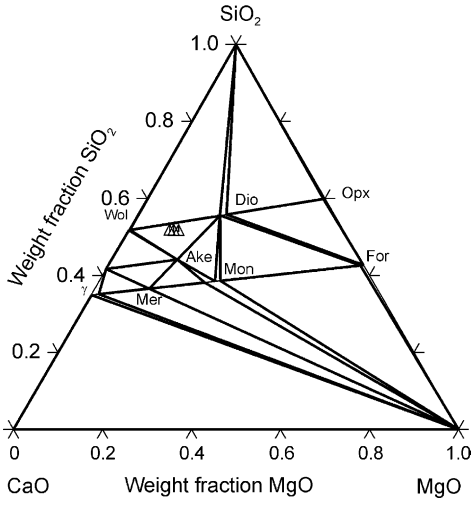

Fig. 8. Isothermal section of the ternary CaO–MgO–SiO_2 diagram at 800 °C. The investigated compositions 1, 2 and 3 are marked with triangles (see the text) (Wol, wollastonite; Dio, diopside; Ake, akermanite; Mer, merwinite; Mon, monticellite; Opx, orthopyroxene; For, forsterite; γ, Ca_2SiO_4 with olivine structure).

Table 4
Calculated proportions of phases formed at thermodynamic equilibrium regime for the investigated compositions 1, 2 and 3 at 800 °C if we neglect B_2O_3, P_2O_5, Na_2O and CaF_2 (in wt.%)

Composition	Diopside	Akermanite	Wollastonite
1	40.50	25.84	33.66
2	36.32	23.35	40.33
3	32.94	21.21	45.85

regime at 800 °C. These results agree fairly well with the results of the X-ray analysis made in the glass-powder compacts heat treated at 750 °C and 800 °C (Fig. 6).

This agreement suggests that there is no influence of B_2O_3, P_2O_5, Na_2O and CaF_2 on the products of crystallization of the investigated parent glasses, at least within in the range of the amounts used, although crystallization started at relatively lower temperatures that those usually reported in these systems.[2,4] However, earlier studies have demonstrated that these compounds play an important role in lowering the melting point of the glasses and in enhancing sinterability.[19,22,23] Although viscosity measurements were not carried out in the present study, the achievement of good properties for the glass–ceramics sintered at relatively low temperatures (700–800 °C, Tables 2 and 3) supports such a role of these compounds.

As far as sintering is concerned, the experimental results showed that densification of glass-powder compacts starts at 620–625 °C, it advances at higher temperatures, likely by viscous flow sintering, and it is almost completed at 700 °C. Crystallization starts at temperatures >700 °C. Crystallinity increases at higher temperatures (750 °C, 800 °C), resulting in fully dense glass–ceramic materials, which are predominantly composed of diopside and wollastonite together with small amounts of akermanite and residual glassy phase (Fig. 6).

Karamanov et al. have proposed that the crystallization of diopside may cause formation of additional porosity since there is a significant difference between the density of diopisde in glassy (2.75 g/cm^3) and crystal state (3.27 g/cm^3).[36] Note that the difference of density is negligible in the case of wollastonite (2.87 g/cm^3 and 2.92 g/cm^3 for the glass and the crystals, respectively).[37] The effect of this phenomenon was obvious in the crystallization of the bulk glasses (i.e. formation of big pores in the core of the bulk samples, Fig. 1d). The experimental results show that processing of glass–ceramics using glass-powder compacts considerably suppressed the effect of this deleterious phenomenon and uniform crystallization seemingly occurred over the entire bulk of the glass-powder compacts. Certainly, small amount of micropores should remain in the intergranular spaces of the crystals in the glass–ceramics due to the aforementioned difference of density during crystallization, which should be reflected in the slight decrease of density of the samples heat treated at 800 °C comparing to the properties at 750 °C (Table 2), which was more pronounced at higher temperatures (i.e. >800 °C).

Compositions 2 and 3, which contains the lowest amount of fluxes, exhibits the best mechanical properties (Table 2). The measured bending strength of the samples heat treated at 800 °C, which ranged between 116 MPa and 141 MPa, was higher than the values reported for powder compacts made of glasses of other compositions (usually lower than 100 MPa).[4,17,38,39] Toya et al. have proposed that diopside is a preferable crystalline phase since it results in stronger materials than glass–ceramics based on wollastonite or anorthite.[17,38]

The values of microhardness and thermal expansion coefficient of the produced glass–ceramics at 800 °C (Table 3) as well as their aesthetic characteristics (Fig. 5) indicate that they may be potential candidates for biomedical applications.[1,40] In a forthcoming article, we shall present the properties of these materials with regard to their potential use in biomedical applications (i.e. dental and bone substitutes).

With regards to environmental and economical issues, in this study the melting of glasses (1400 °C, 1 h) and the production of high quality glass–ceramics (750–800 °C) occurred at temperatures lower than those used in other similar cases reported in literature. For instance, wollastonite glass–ceramics are produced in large scale for commercial use as cladding materials for the building industry in Japan. The processing involves first melting of the base glass in a tank furnace at 1500 °C and then crystallization of coarse (1–7 mm long) glass-grains to β-wollastonite at 1100 °C for 2 h.[1] In a recent work on pyroxene-based glass–ceramic glazes, based on the quaternary $CaO–MgO–Al_2O_3–SiO_2$ system and containing small amounts of B_2O_3, Na_2O and K_2O, the parent glasses were melted at 1600 °C and crystallized to pyroxene phases at temperatures ≥900 °C.[19] In the $CaO–MgO–SiO_2$ system, glass–ceramics of diopside–wollastonite have been prepared by melting of the parents glasses at 1500 °C for 3 h.[41]

Beyond the effect of viscosity, the choice of the composition of the basic glass in the $CaO–MgO–SiO_2$ system and the overall effect of B_2O_3, P_2O_5, Na_2O and CaF_2, as they were used in the present study, probably result in a multi-component system whose excess of free energy related to chemical gradient favours diffusion and enhances sintering.[42,43]

The results of this study can be explored for the improvement of the technology and the properties of glass–ceramics and glass–ceramic glazes and to decrease their production cost. Moreover, the investigated compositions can be used as models for vitrification and ceramization of industrial and municipal wastes, provided that further durability and leaching tests of the produced glasses and glass–ceramics are carried out.[7,44,45]

5. Conclusions

The production of glass–ceramics based on the $CaO–MgO–SiO_2$ system using additives B_2O_3, P_2O_5, Na_2O

and CaF_2 confirmed the importance of correct selection of parent glass composition to achieve low production cost of materials with high quality. The basic compositions of the parent glasses were selected to be as 51–52% SiO_2, 37–39% CaO and 9–12% MgO, which are located in the field of primary crystallization of pseudowollasotine phase in the ternary CaO–MgO–SiO_2 system and close to the composition of the liquid in the invariant equilibrium of the transition and eutectic type, described by Eqs. (1) and (2), respectively.

The obtained results are summarized as follows:

1. Transparent and colourless glasses were prepared via melting of the batches at 1400 °C for 1 h followed by annealing at 600 °C. The main constituents of the glass-network are the units Q^1 and Q^2. The glasses feature clear evidence of liquid–liquid phase separation.
2. The microstructure of the bulk glasses heat treated at 800 °C indicated that the investigated glasses are prone to surface crystallization. Crystal growth advanced from the surface towards the core of the bulk glass. Crystallization was completed at 900 °C.
3. Completely dense samples of dark grey colour but of amorphous nature were obtained after heat treatment of glass-powder compacts at 700 °C, indicating that sintering precedes crystallization. Devitrification started at higher temperatures (>700 °C). White and highly dense materials were obtained after heat treatment at 750 °C and 800 °C. X-ray analysis confirmed formation of diopside, wollastonite, as principal phases, and akermanite. Thermodynamic calculations in the ternary CaO–MgO–SiO_2 system at 800 °C anticipate the formation of exactly the same assemblage of phases.
4. The glass–ceramics heat treated at 800 °C exhibited bending strength of 116–141 MPa, Vickers microhardness of 4.53–4.65 GPa and thermal expansion coefficient (100–500 °C) of 9.4–10.8 × 10^{-6} K^{-1}.
5. The results of this study can be explored for the improvement of the technology and the properties of glass–ceramics and glass–ceramic glazes. The decrease of production cost due to the reduction of processing temperature with no compromise of the quality of the produced materials is also an interesting feature.

Acknowledgements

This study was supported by CICECO and the Portuguese FCT.

References

1. Höland, W. and Beall, G., *Glass–Ceramic Technology*. The American Ceramic Society, Westerville, OH, 2002.
2. Pavlushkin, N. M., *Principals of Glass Ceramics Technology* (*2nd ed.*). Stroiizdat, Moscow, 1979 (in Russian).
3. McMillan, P. W., *Glass–Ceramics*. Academic Press, London, 1964.
4. Strnad, Z., *Glass–Ceramic Materials*. Elsevier, Amsterdam, 1986.
5. Zhunina, L. A., Kuzmenkov, M. I. and Yaglov, V. N., *Pyroxene Glass–Ceramics*. University of Minsk, 1974 (in Russian).
6. Fredericci, C., Zanotto, E. D. and Ziemath, E. C., Crystallization mechanism and properties of blast furnace slag glass. *J. Non-Cryst. Solids*, 2000, **273**, 64–75.
7. Barbieri, L., Bonamartini, I. and Lancellotti, I., Alkaline and alkaline earth silicate glasses and glass–ceramics form municipal and industrial wastes. *J. Eur. Ceram. Soc.*, 2000, **20**, 2477–2483.
8. Oevecoglu, M. L., Kuban, B. and Ozer, H., Characterization and crystallization kinetics of diopside based glass–ceramic developed from glass industry raw materials. *J. Eur. Ceram. Soc.*, 1996, **17**, 957–962.
9. Alizadeh, P. and Marghussian, V. K., Effect of nucleating agents on the crystallization behaviour and mirostucture of SiO_2–CaO–MgO(Na_2O) glass–ceramics. *J. Eur. Ceram. Soc.*, 2000, **20**, 775–782.
10. Karamanov, A., Pisciella, P. and Pelino, M., The effect of Cr_2O_3 a nucleating agent in iron rich glass–ceramics. *J. Eur. Ceram. Soc.*, 1999, **19**, 2641–2645.
11. Karamanov, A., Castalini, C., Pelino, M. and Hreglich, A., Kinetics of phase formation in Jarosite glass–ceramics. *J. Eur. Ceram. Soc.*, 1999, **19**, 527–533.
12. Zhunina, L. A., Nucleated crystallization of glasses in pyroxene systems. *Nucleated Crystallization of Glasses*. State Institute of Glass, Moscow, 1982, pp. 12–21 (in Russian).
13. Zhunina, L. A., The ways of controlled mineralization in pyroxene systems issue 9. *Glasses, Glass–Ceramics and Silicates*. Belarus Academy of Sciences, Minsk, 1979, pp. 65–69 (in Russian).
14. Tulyaganov, D. U., Agathopoulos, S., Kharton, V. V. and Marques, F. M. B., Glass–ceramics in the former Soviet Union: a review on industry-oriented developments. *Ind. Ceram.*, 2003, **23**, 101–115.
15. Sarkisov, P. D., The modern state of technology and application of glass–ceramics. In *Proceedings of the XI International Congress on Glass*. Society of Glass Technology, Sheffield, 1989. pp. 411–441.
16. Beall, G. H., Glass–ceramics: recent developments and applications. *Ceram. Trans.*, 1993, **30**, 241–266.
17. Toya, T., Kameshima, Y., Yasumori, A. and Okada, K., Preparation and properties of glass–ceramic clay wastes (kira) of silica and kaolin clay refining. *J. Eur. Ceram. Soc.*, 2004, **24**, 2367–2372.
18. Kokubo, T., Ito, S., Sakka, S. and Yamamuro, T., Formation of high-strength bioactive glass–ceramic in the system MgO–CaO–SiO_2–P_2O_5. *J. Mater. Sci.*, 1986, **21**, 536–540.
19. Torres, F. J. and Alarcon, J., Mechanism of crystallization of pyroxene-based glass–ceramic glazes. *J. Non-Cryst. Sol.*, 2004, **34**, 45–51.
20. Baldi, G., Generlli, E. and Leonelli, C., Effects of nucleating agents on diopside crystallization in new glass–ceramics for tile gaze application. *J. Mater. Sci.*, 1995, **30**, 3251–3255.
21. Ernest, M. L., Robbins, C. R. and McMurdie, H. F., *Phase Diagrams for Ceramists*. American Ceramic Society Inc., Westerwille, OH, 1994.
22. Shyu, J. J. and Lee, H. H., Sintering crystallization and properties of B_2O_3/P_2O_5 doped $Li_2O{\cdot}Al_2O_3{\cdot}4SiO_2$ glass–ceramics. *J. Am. Ceram. Soc.*, 1995, **78**, 2161–2167.
23. Tulyaganov, D. U. and Ismatov, A. A., Development and application of anorthite–diopside containing glass–ceramics. *Ceram. Trans.*, 1993, **29**, 221–224.
24. Brawer, S. A. and White, W. B., Raman spectroscopic investigation of structure of silicate-glasses: II. Soda-alkaline earth alumina ternary and quaternary glasses. *J. Non-Cryst. Solids*, 1977, **23**, 261–278.
25. Brawer, S. A. and White, W. B., Raman spectroscopic investigation of structure of silicate-glasses: I. Binary alkali silicates. *J. Chem. Phys.*, 1975, **63**, 2421–2432.
26. Mysen, B. O., Virgo, D. and Scarfe, C. M., Solubility mechanisms of carbon-dioxide in silicate metals. A Raman spectroscopic study. *Am. Miner.*, 1980, **65**, 885–899.

27. McMillan, P., A Raman-spectroscopic study of glasses in the system CaO–MgO–SiO_2. *Am. Miner.*, 1984, **69**, 645–659.
28. Tatsumisago, M., Minami, T., Umesaki, N. and Iwamoto, N., Raman-spectra of Li_2O–SiO_2 glasses prepared by rapid quenching. *Chem. Lett.*, 1986, **8**, 1371–1374.
29. Mysen, B. O. and Frantz, J. D., Raman-spectroscopy of silicate melts at magmatic temperatures—Na_2O–SiO_2, K_2O–SiO_2 and Li_2O–SiO_2 binary compositions in the temperature-range 25–1475 °C. *Chem. Geol.*, 1992, **96**, 321–332.
30. Kamitsos, E. I., Karakassides, M. A. and Chryssikos, G. D., Structure of borate glasses, part I: Raman study of cesium, rubidium and potassium borate glasses. *Phys. Chem. Glasses*, 1989, **30**, 229–234.
31. Kamitsos, E. I., Karakassides, M. A. and Chryssikos, G. D., A vibrational study of lithium borate glasses with high Li_2O content. *Phys. Chem. Glasses*, 1987, **28**, 203–209.
32. Chryssikos, G. D., Bond length—Raman frequency correlations in borate crystals. *J. Raman Spectrosc.*, 1991, **22**, 645–650.
33. Karakassides, M. A., Saranti, A. and Koutselas, I., Preparation and structural study of binary phosphate glasses with high calcium and/or magnesium content. *J. Non-Cryst. Solids*, 2004, **347**, 69–79.
34. Kukolev, G. V., *Silicon Chemistry and Physical Chemistry of Silicates*. Vyshaya shkola, Moscow, 1966 (in Russian).
35. Huang, W., Hillert, M. and Wang, X., Thermodynamic assessment of CaO–MgO–SiO_2 system. *Met. Mater. Trans.*, 1995, **26A**, 2293–2310.
36. Karamanov, A., Arriza, L., Matekovits, I. and Pelino, M., Properties of sintered glass–ceramics in the diopisde–albite system. *Ceram. Int.*, 2004, **30**, 2119–2135.
37. Karamanov, A. and Pelino, M., Evaluation of degree of crystallization in glass–ceramics by density measurements. *J. Eur. Ceram. Soc.*, 1999, **19**, 649–654.
38. Toya, T., Tamura, Y., Kameshima, Y. and Okada, K., Preparation and properties of CaO–MgO–Al_2O_3–SiO_2 glass–ceramics from kaolin clay refining waste (Kira) and dolomite. *Ceram. Int.*, 2004, **30**, 983–989.
39. Tulyaganov, D. U., Ribeiro, M. J. and Labrincha, J. A., Development of glass–ceramics by sintering and crystallization of fine powder of calcium–magnesium–aluminosilicate glass. *Ceram. Int.*, 2002, **28**, 515–520.
40. Höland, W., Biocompatible and bioactive glass–ceramics: state of the art and new directions. *J. Non-Cryst. Solids*, 1997, **219**, 192–197.
41. Abdel-Hameed, S. A. M. and El-kheshen, A. A., Thermal and chemical properties of diopside–wollastonite glass–ceramics in the SiO_2–CaO–MgO system from raw materials. *Ceram. Int.*, 2003, **29**, 265–269.
42. German, R. M., *Powder Metallurgy Science* (*2nd ed.*). Metal Powder Industries Federation, New Jersey, 1994, pp. 268–269.
43. Lira, C., Novaes de Oliveira, A. P. and Alarcon, O. E., Sintering and crystallization of CaO–Al_2O_3–SiO_2 glass powder compacts. *Glass Technol.*, 2001, **42**, 91–96.
44. Barbieri, L., Lancellotti, I., Manfredini, T., Queralt, I., Rincon, J. and Romeiro, M., Vitrification of fly ash from thermal power stations. *Glass Technol.*, 1997, **38**, 165–170.
45. Gutman, R., Thermal technologies to convert solid–solid wastes residuals into technical glass products. *Glastech. Ber. Glass Sci. Technol.*, 1996, **69**, 285–299.